Journal of Microbiology (2015) Vol. 53, No. 11, pp. 783–795
DOI 10.1007/s12275-015-5333-8

The *Mycobacterium tuberculosis relBE* toxin:antitoxin genes are stress-responsive modules that regulate growth through translation inhibition

Shaleen B. Korch[1,2*], Vandana Malhotra[1], Heidi Contreras[1#], and Josephine E. Clark-Curtiss[1,3]

[1]*Center for Infectious Diseases and Vaccinology, Biodesign Institute, Arizona State University, Tempe, Arizona 85287, USA*
[2]*Department of Pharmacology, Midwestern University, Glendale, Arizona 85308, USA*
[3]*School of Life Sciences, Arizona State University, Tempe, Arizona 85287, USA*
[#]*Present address: Department of Molecular Biology and Biochemistry, University of California, Irvine, California, 92697, USA*

(Received Jul 2, 2015 / Revised Sep 30, 2015 / Accepted Oct 5, 2015)

Toxin-antitoxin (TA) genes are ubiquitous among bacteria and are associated with persistence and dormancy. Following exposure to unfavorable environmental stimuli, several species (*Escherichia coli*, *Staphylococcus aureus*, *Myxococcus xanthus*) employ toxin proteins such as RelE and MazF to downregulate growth or initiate cell death. *Mycobacterium tuberculosis* possesses three Rel TA modules (Rel_{Mtb}): $RelBE_{Mtb}$, $RelFG_{Mtb}$ and $RelJK_{Mtb}$ (Rv1246c-Rv1247c, Rv2865-Rv2866, and Rv3357-Rv3358, respectively), which inhibit mycobacterial growth when the toxin gene (*relE*, *relG*, *relK*) is expressed independently of the antitoxin gene (*relB*, *relF*, *relJ*). In the present study, we examined the *in vivo* mechanism of the $RelE_{Mtb}$ toxin protein, the impact of $RelE_{Mtb}$ on *M. tuberculosis* physiology and the environmental conditions that regulate all three rel_{Mtb} modules. $RelE_{Mtb}$ negatively impacts growth and the structural integrity of the mycobacterial envelope, generating cells with aberrant forms that are prone to extensive aggregation. At a time coincident with growth defects, $RelE_{Mtb}$ mediates mRNA degradation *in vivo* resulting in significant changes to the proteome. We establish that rel_{Mtb} modules are stress responsive, as all three operons are transcriptionally activated following mycobacterial exposure to oxidative stress or nitrogen-limiting growth environments. Here we present evidence that the rel_{Mtb} toxin:antitoxin family is stress-responsive and, through the degradation of mRNA, the $RelE_{Mtb}$ toxin influences the growth, proteome and morphology of mycobacterial cells.

Keywords: *Mycobacterium tuberculosis*, growth, *relBE*, stress, toxin:antitoxin, mRNA

*For correspondence. E-mail: skorch@midwestern.edu; Tel.: +1-623-572-3708; Fax:+1-623-572-3648

Introduction

Mycobacterium tuberculosis has the unique ability to persist for long periods of time in its host as a latent infection. Despite all efforts, the molecular switch(es) governing *M. tuberculosis*' growth rate are still unknown. Toxin-antitoxin (TA) modules have the potential to act as master regulators of *M. tuberculosis* growth. These bi-cistronic modules are divided into five classes based on genetic architecture and the mode of TA regulation but have in common a toxin component (protein) and an antitoxin component (protein or RNA), which is responsible for neutralizing the toxin's effect (Fozo *et al.*, 2010; Leplae *et al.*, 2011; Blower *et al.*, 2012). In the absence of their cognate antitoxin, toxin proteins interfere with macromolecular processes resulting in the inhibition of growth and, in some cases, the generation of antibiotic-tolerant persister cells (Korch and Hill, 2006; Singh *et al.*, 2010; Germain *et al.*, 2013; Maisonneuve and Gerdes, 2014; Tripathi *et al.*, 2014). Curiously, the genome of *M. tuberculosis* has a remarkable number of putative TA loci (>80), far more than other prokaryotes (Arcus *et al.*, 2005; Ramage *et al.*, 2009). The physiological role(s) and overall benefits of having such a large repertoire of TA loci are unknown. However, given the redundancy in TA loci throughout the genome (i.e., 45 *vapBC* loci), it is easy to speculate that these modules are critically important to *M. tuberculosis*' pathogenicity and could play a role in the regulation of *M. tuberculosis* growth and/or persistence. Recently, Tiwari *et al.* (2015) demonstrated that three $MazF_{Mtb}$ toxin proteins play a synergistic role in *M. tuberculosis* drug tolerance and virulence in guinea pigs.

Historically, TA modules were identified based on their role in plasmid stability, ensuring stable plasmid inheritance in growing populations through a postsegregational killing mechanism of daughter cells that failed to inherit the parent plasmid (Orgura and Hiraga, 1983; Gerdes *et al.*, 1986; Tsuchimoto *et al.*, 1988; Jensen and Gerdes, 1995). Recent analysis has revealed additional and seemingly contradictory roles for chromosomally encoded TA modules: programmed cell death (PCD) and programmed cell survival (PCS). Programmed cell death is described as an "altruistic" cell suicide program, where toxin-induced death of a percentage of cells within a population aids in the survival of the remaining population (Engelberg-Kulka *et al.*, 2006), or alternatively, functions as part of an obligatory cell lysis program in the life cycle of a population [e.g., *Myxococcus xanthus* (Nariya and Inouye, 2008)]. On the other hand, PCS is described as a stress response mechanism, whereby toxin

proteins enable cells to transit into a non-growing, persister state during periods of unfavorable growth conditions, with growth resumption following removal of the stress (Korch *et al.*, 2003; Gerdes *et al.*, 2005; Pandey and Gerdes, 2005; Korch and Hill, 2006). In an elegant analysis of the *E. coli* MazF toxin, Amitai and colleagues brought the concepts of PCD and PCS together by demonstrating that the MazF toxin contributes to the simultaneous synthesis of both "survival" and "death" proteins following exposure to the DNA damaging agent nalidixic acid, or a translation inhibitor, spectinomycin (Amitai *et al.*, 2009). Thus, the PCD and PCS programs are not necessarily mutually exclusive, but rather, bacteria seem to have the option of one or the other or both, which is probably dependent upon the species, TA module and environmental stimuli.

Extensive analysis of Type II toxins has revealed toxin activities including translation inhibition through mRNA cleavage [RelE (Christensen and Gerdes, 2003; Pedersen *et al.*, 2003; Neubauer *et al.*, 2009; Hurley *et al.*, 2011; Goeders *et al.*, 2013), MazF (Christensen *et al.*, 2003; Zhang, 2003; Nariya and Inouye, 2008; Fu *et al.*, 2009), HigB (Hurley and Woychik, 2009), YoeB (Christensen-Dalsgaard and Gerdes, 2008; Zhang and Inouye, 2009), YafQ (Prysak *et al.*, 2009), MsqR (Yamaguchi *et al.*, 2009)], initiator $tRNA^{fMet}$ cleavage [$VapC_{E.coli}$, (Winther and Gerdes, 2011; Lopes *et al.*, 2014)], or cleavage of 23S rRNA [$VapC20_{Mtb}$, (Winther *et al.*, 2013) and MazF-mt6, (Schifano *et al.*, 2013)] or 16S rRNA [MazF-mt3, (Schifano *et al.*, 2014)], as well as DNA replication inhibition through DNA gyrase interference [ParE, (Jiang, 2002; Hallez *et al.*, 2010)], or phosphorylation of glutamyl-tRNA synthetase [HipA, (Germain *et al.*, 2013; Kaspy *et al.*, 2013)]. In *E. coli*, the RelE toxin ($RelE_{E.coli}$) has mRNA interferase activity, preferentially cleaving UAA and UAG stop codons (Christensen and Gerdes, 2003) and sense codons UCG and CAG (Christensen and Gerdes,, 2003; Pedersen *et al.*, 2003) *in vitro*. In contrast, *in vivo* analysis revealed less discriminating toxin activity, as $RelE_{E.coli}$ cleaved within the first 100 codons of transcripts, regardless of codon sequence (Hurley *et al.*, 2011). The differential enzymatic activity of $RelE_{E.coli}$ between *in vitro* and *in vivo* conditions is possibly due to co-factors present *in vivo* that direct or influence $RelE_{E.coli}$ activity. The MazF toxin possesses mRNase activity in *E. coli*, *Staphylococcus aureus*, and *M. tuberculosis*. Although MazF in all three species cleaves mRNA, the recognition sequences are significantly different: $MazF_{E.coli}$ cleaves at the 5′-end of ACA sequences (Zhang, 2003, 2005) and at the 5′ side of residue A in 5′-NAC-3′ sequences (where N is preferentially U or A) (Muñoz-Gómez *et al.*, 2004); $MazF_{S. aureus}$ cleaves an abundant pentad sequence, U*ACAU (Zhu *et al.*, 2009); MazF-mt3, MazF-mt6, and MazF-mt7 (*M. tuberculosis*) target CU*CCU/UU*CCU, UU*CUU and U*CGCU, respectively (Zhu, 2008; Schifano *et al.*, 2013), (* indicates the cleavage site). Clearly, specific cellular targets of toxin proteins are toxin- and species-dependent.

The goal of the current study was to better understand the role of $relBE_{Mtb}$ in mycobacterial physiology and its contribution towards mycobacterial growth adaptation. Over expression of $relE_{Mtb}$ in the absence of its cognate antitoxin in *M. smegmatis* potentiated two alternate phenotypes within a genetically identical population: (1) atypical cell shape and (2) increase in cell surface "stickiness", both suggesting alterations in mycobacterial envelope composition as a consequence of increased cellular levels of the toxin. Contemporaneous with morphological changes, over expression of $relE_{Mtb}$ in *M. smegmatis* resulted in an altered proteome and mRNA cleavage. Finally, an analysis of *relBE*, *relFG*, and *relJK* expression revealed that all three rel_{Mtb} gene pairs are transcriptionally regulated in *M. tuberculosis* in response to environmental cues such as hypoxia, oxidative stress and nitrogen limiting conditions.

Materials and Methods

Media and chemicals

M. tuberculosis H37Rv was grown at 37°C in Middlebrook 7H9 liquid medium or on Middlebrook 7H10 agar (Difco) supplemented with ADS (0.5% bovine serum albumin-fraction V, 0.2% dextrose, 0.85% saline) enrichment and 0.05% Tween 80 (Tw). For stress response studies, appropriate media adjustments were made as described below. *M. smegmatis* mc^2155 was grown with aeration at 37°C in Middlebrook 7H9 liquid medium (Difco) supplemented with 0.05% Tw or on Luria-Bertani (LB) agar plates (Sambrook, 1989). *E. coli* was grown in LB broth or on LB agar plates at 37°C. The following concentrations of antibiotics or inducing supplement were added when appropriate: kanamycin (Kan), 50 μg/ml;

Table 1. Strains and plasmids used in this study

Strain	Relevant features	Source or reference
M. tuberculosis H37Rv	Virulent laboratory strain	ATCC
M. smegmatis mc^2155	*ept-1*	Snapper (1990)
E. coli JM109	$e14^-$ ($McrA^-$) *recA1 endA1 gyrA96 thi-1 hsdR17 supE44 relA1* Δ(*lac-proAB)*	Stratagene
LIX32	mc^2155 with pYA1611	Korch *et al.* (2009)
LIX33	mc^2155 with pYA1611::$relE_{Mtb}$	Korch *et al.* (2009)
LIX34	mc^2155 with pYA1611::$relBE_{Mtb}$	Korch *et al.* (2009)
Plasmids		
pYA1611	*tetR* gene in *Not*I site of pSE100	Korch *et al.* (2009)
pYA1611::$relE_{Mtb}$	$relE_{Mtb}$ gene in *Pst*I site of pYA1611	Korch *et al.* (2009)
pYA1611::$relBE_{Mtb}$	$relBE_{Mtb}$ gene in *Pst*I site of pYA1611	Korch *et al.* (2009)
pYA1655	*M. smegmatis gly* in *Hin*dIII/*Sac*I sites of pET28a(+)	This study
pYA1656	*M. smegmatis zbpA* in *Hin*dIII/*Sac*I sites of pET28a(+)	This study

hygromycin (Hyg), 50 μg/ml; ampicillin (Amp), 100 μg/ml and anhydrotetracycline (ATc), 100 ng/ml.

Strains and plasmids

E. coli strain JM109 was used as a host for plasmid constructions (Stratagene). *M. tuberculosis* H37Rv (ATCC no. 25618) and *M. smegmatis* mc^2155 (obtained from William R. Jacobs, Jr., Albert Einstein College of Medicine, New York, NY) were used in the present study. For over expression experiments, pYA1611, pYA1611::*relE*, and pYA1611::*relBE* were used. The pYA1611 series of vectors allow for the controlled and inducible expression of *relE* and *relB* genes, as previously described (Korch *et al.*, 2009). Briefly, pYA1611 possesses a TetR-controlled expression system with a $P_{myc}1$*tetO* promoter to drive gene expression; in the absence of anhydrotetracycline (ATc), gene expression is repressed whereas in the presence of ATc, ATc binds the TetR protein resulting in TetR dissociation from *tetO*, thereby allowing induction of gene expression. In all assays, ATc was used to induce gene expression as it has a high affinity to TetR and low toxicity and thus had no measurable effect on the viability of *M. smegmatis*.

Detailed plasmid constructions are available upon request to S. B. Korch. Table 1 summarizes the mycobacterial strains and plasmids used for the studies presented here.

Fluorescence microscopy

A LIVE/DEAD BacLight bacterial viability kit (Invitrogen) was used to determine the proportion of cells that retained membrane integrity, and presumably viability, after over expression of $relE_{Mtb}$ alone or when co-expressed with $relB_{Mtb}$. Overnight cultures of *M. smegmatis* LIX32 (empty vector), LIX33 (pYA1611::*relE*) and LIX34 (pYA1611::*relBE*) were diluted to an OD_{600} of 0.01 in 7H9 supplemented with Tw and Hyg. Cultures were grown at 37°C. At an OD_{600} of 0.1, cultures were split, the cells were washed with pre-warmed 7H9, resuspended in 7H9-Tw-Hyg and to one culture 100 ng/ml ATc was added to induce $relE_{Mtb}$ (LIX33) or $relBE_{Mtb}$ (LIX34) expression, while the second culture served as the uninduced control. Following the addition of ATc (induction of $relE_{Mtb}$ or $relBE_{Mtb}$) to the media, 300 μl samples were removed at specific time points, concentrated by centrifugation for 2 min at 14,000 rpm in an Eppendorf microcentrifuge, and resuspended in 300 μl of 0.85% NaCl. Then, 1 μl of SYTO-9-propidium iodide (PI) mix (1:1 ratio) was added to 300 μl of cell suspension and incubated in the dark for 15 min prior to photography. Phase-contrast and fluorescence microscopy were performed with a Nikon Optiphot 2 microscope. Random fields (>50) were photographed with a Pixera 600CL CCD digital camera. Triplicate cultures were analyzed.

To quantify the live/dead sub-populations of cells within a culture, at specific time points LIX32 and LIX33 aliquots were removed and subjected to aspiration to break up cell aggregates to produce a single cell suspension. Briefly, cultures were aspirated using a 20 G needle then expelled slowly using a 30 G needle. Sufficient dissociation of clumps was achieved following seven aspirations. Samples were processed and stained with SYTO-9-PI as described above and quantification of live and dead cells was achieved using a SpectraMax M2 (Molecular Devices) with an excitation of 485 and emission of 530 (live, green) and 630 (dead, red). The percentage of live/dead cells was calculated from a standard curve prepared by mixing live (0.85% saline-exposed) and dead (40% isopropanol-exposed) *M. smegmatis* together at various proportions of live:dead cells (100%, 75%, 50%, 25%, 0% alive).

Growth and pulse-chase labeling

To determine whether $RelE_{Mtb}$ affects macromolecular synthesis, pulse-chase experiments were conducted on *M. smegmatis* strains LIX32 (pYA1611), LIX33 (pYA1611::$relE_{Mtb}$) and LIX34 (pYA1611::$relBE_{Mtb}$). Cells were grown as described for fluorescent microscopy. At specific time points, three 500 μl samples were removed and one of each was labeled with [^{35}S]methionine (1 μCi; 1175 Ci/mmol) for 15 min, [^{3}H]thymidine (1 μCi; 20 Ci/mmol) for 15 min, or [^{3}H]uridine (0.1 μCi; 27 Ci/mmol) for 15 min at 37°C. Samples were chased at 37°C for 1 h with 100 μg of cold methionine/ml, 1 mg of cold thymidine/ml, or 1 mg of cold uridine/ml. Aliquots of 500 μl of labeled cells were added to 1 ml of precipitation solution (90 ml of 0.5 N NaOH plus 10 ml of carrier mix [5 μg of lysozyme/ml, 20 μg of salmon sperm DNA/ml, and 10 μg of bovine serum albumin/ml in 0.5 N NaOH]) and vortexed, and then 1 ml of ice-cold 20% trichloroacetic acid (TCA) was added. Samples were placed on ice for 30 min, and precipitates were collected on Whatman GF/C filters (Whatman) prewet with 10% TCA. Samples on the filters were washed twice with 2 ml of ice-cold 10% TCA, once with 3 ml of ice-cold 95% ethanol, dried, and counted in 5 ml of scintillation fluid (EcoLume, Cardinal Health).

Protein preparation for 2 dimensional (2D) protein analysis

LIX33 was grown as described for the fluorescent microscopy experiments. At specific time points, 25 ml of culture was prepared for 2D gel protein analysis using the ReadyPrep Protein Extraction Kit (Bio-Rad Laboratories). Briefly, the cells were pelleted by centrifugation and washed with 1× phosphate buffered saline (PBS), then resuspended in 1 ml 2D-rehydration buffer (Bio-Rad). The cells were mechanically lysed with 0.1 mm Zirconia beads by using a FastPrep FP120 bead beater, with three 45 sec pulses separated by 1 min cooling on ice between each pulse. Cell lysates were centrifuged, and the supernatant collected as whole cell lysate. All protein samples were cleaned to remove contaminants (e.g., salts, lipids) prior to 2D analysis using the 2D Clean Up Kit according to the manufacturer's instructions (GE Health Care Amersham). Protein samples were analyzed using 11 cm pH 4–7 immobilized pH gradient strips (Bio-Rad Laboratories) using active rehydration over night at 50 volts. The proteins in the sample were separated in the first dimension by isoelectric focusing carried out at 40 kVh. In the second dimension, proteins were separated on vertical 8–16% Tris-HCl Criterion gels (Bio-Rad Laboratories). Protein gels were fixed and stained with Sypro Ruby, imaged, and overlays of the gels made using Z3 gel analysis software (Compugen). Protein identification was performed on protein spots excised from Sypro Ruby stained gels, followed

by digestion with trypsin. Peptides were eluted and peptide sequences were determined by tandem mass spectrometry (MS/MS). Each mass spectrometry spectrum was searched against a protein sequence data base (NCBI, Swiss Protein), resulting in a set of tryptic peptide matches with 99% confidence.

In vitro transcription/translation

The *E. coli* T7 S30 Extract System for Circular DNA (Promega) was used for *in vitro* translation assays. Reaction mixtures (25 µl) were prepared according to the manufacturer's instructions using [^{35}S]methionine (>1,000 Ci/mmol; Amersham). For each reaction, pET11::*relB*$_{Mtb}$, pET11::*relE*$_{Mtb}$ or pET28a(+) vector containing the appropriate *M. smegmatis* gene (*gly*, *zbpA*, *fabG*, *thioredoxin*) served as the DNA template and was added in 0.5- to 1.0-µg amounts. For independent analysis of *gly*, *zpbA*, *fabG*, and *thioredoxin* transcripts, the reaction mix plus DNA template was gently vortexed, incubated at 37°C for 2 h, and then transferred to ice for 5 min. For analysis of the effects of RelE or RelB on transciption/translation, pET11::*relB* and/or pET11::*relE* was added to the reaction mix, gently vortexed, and incubated at 37°C for 30 min. Following incubation, pET11::*gly*/*fabG*/*zbpA*/*thioredoxin* was added to the reaction mix, gently vortexed, and incubated at 37°C for an additional 1.5 h, and then transferred to ice for 5 min. For sodium dodecyl sulfate-polyacrylamide gel electrophoresis (SDS-PAGE) analysis, 5 µl of the T7 S30 reaction was added to 20 µl of acetone. Samples were incubated on ice for 15 min, spun at 12,000 × *g* for 5 min, resuspended in 20 µl of SDS-PAGE sample buffer, and boiled for 5 min. Aliquots were analyzed by SDS-PAGE on a 15% polyacrylamide gel. Detailed construction of plasmids can be obtained from S.B. Korch.

RNA isolation

M. smegmatis strains LIX32 and LIX33 were grown as described above for fluorescent microscopy experiments. At specific points, total RNA was isolated from *M. smegmatis* cultures using TRI reagent (Ambion Inc.) according to the manufacturer's protocol and as previously described (Malhotra *et al.*, 2009). The quality of RNA was assessed using the Experion system (Bio-Rad Laboratories) and the concentration determined using an ND-1000 spectrophotometer (Thermo Scientific).

To assess whether specific transcripts were present following *relE*$_{Mtb}$ over expression, total RNA isolated from LIX32 and LIX33 cells 24 h post induction was converted to cDNA by RNase H$^+$ MMLV reverse transcriptase using an iScript cDNA synthesis kit (Bio-Rad Laboratories) according to the manufacturer's instructions. cDNAs were PCR amplified using primer pairs that would amplify the entire gene. The following primer pairs were used for amplification:; *zbpA*, forward: 5′-CGCGGAGCTCGTGAAAGTCTTCGAC-3′ and reverse: 5′-CGCGAAGCTTTCAGCCGATGAAGCG-3′, and *glyoxylase*, forward: 5′-CGCGGAGCTCATGAGTGACCACGAA-3′ and reverse: 5′-CGCGAAGCTTTCAGCGCTTGAGCGG-3′. For each amplification, RNA without reverse transcriptase served as a negative control to exclude amplification from DNA contamination in the sample. Semiquantitative RT-PCR analysis was done for *relE*, *gly*, and *zbpA* transcripts post normalization with 16S rRNA. All amplification products were separated on a 1% agarose gel to determine product size.

Primer extension

A primer that annealed approximately 150 nt downstream from the translational start site of the *gly* gene (*gly*, 5′-TTGATGCCGACCACCACCTT-3′) was end-labeled by incubation with [γ-^{32}P]ATP using T4 polynucleotide kinase. Reverse transcription reactions were carried out with 4 pmol of labeled primer, 10 µg of LIX32 or LIX33 total RNA (growth and isolation described above), and Superscript III reverse transcriptase (Invitrogen). Primer extension reactions were performed using at least two independently isolated RNA samples. Dideoxynucleotide sequencing reactions were performed using the SequiTherm EXCEL II DNA sequencing kit (Epicenter Technologies) according to the manufacturer's instructions, and used the same end-labeled primers used in the reverse transcriptase reactions, and plasmids pYA1655 and pYA1656 as the DNA templates. Sequencing products were separated by electrophoresis in parallel with the primer extension reactions on 8% polyacrylamide, 7.0 M urea, 1.0 × TBE gels.

Growth of *M. tuberculosis* under stress conditions

M. tuberculosis H37Rv cultures (OD_{600}=0.2–0.4) were harvested, washed with Middlebrook 7H9 basal medium (minus ADS supplement), and resuspended in stress-specific medium. For acid stress, the cultures were resuspended in Middlebrook 7H9-Tween 80-ADS medium with the pH adjusted to 5.5. For carbon stress, cultures were resuspended in Middlebrook 7H9-Tween 80-Albumin-NaCl medium (without dextrose). For nitrogen stress, cultures were resuspended in Middlebrook 7H9-Tween 80-ADS medium supplemented with 200 µM L-methionine S-sulfoximine (MSX) (Harth, 1999; Amon *et al.*, 2008a). Methionine sulfoximine inhibits extracellular glutamine synthetase activity which consequently affects nitrogen metabolism (Amon *et al.*, 2008a). Treated and untreated control cultures were grown aerobically for 4 h and 4 d followed by RNA isolation as described below. For hypoxia, *M. tuberculosis* cultures were grown in Dubos-Tween 80-Albumin medium to OD_{600} ~ 0.6 and subjected to hypoxia in sealed tubes for 24 and 48 h as described previously (Saini *et al.*, 2004). For oxidative stress, *M. tuberculosis* was grown as previously described (Malhotra *et al.*, 2010).

Results

RelE$_{Mtb}$ initiates cell envelope aberrations, altered cell morphology and reduces viability

Our previous studies have demonstrated that over-expression of *relE*$_{Mtb}$ drastically inhibits mycobacterial growth (Korch *et al.*, 2009). Given the debate on cell death or dormancy, we sought to determine the viability of mycobacterial cells following *relE*$_{Mtb}$ expression using fluorescence microscopy. The use of *M. smegmatis* as a host for *relE*$_{Mtb}$

expression in our studies provides an advantage that ensures that the observed results are solely attributable to $RelE_{Mtb}$ and not due to cross-interactions between $RelE_{Mtb}$ and its antitoxin, or *relFG* and *relJK* (Yang *et al.*, 2010) or other TA proteins.

To examine the morphology and membrane integrity (as an indicator of viability) of *M. smegmatis* cells after expression of $relE_{Mtb}$, we used a LIVE/DEAD bacterial assay. This assay relies on two dyes that intercalate into DNA: SYTO-9, which penetrates cell membranes and fluoresces green, and propidium iodide (PI), which can only penetrate permeabilized membranes and fluoresces red. When used together, PI lowers SYTO-9 emission causing bacterial cells with intact membranes to fluoresce green ("live") and bacterial cells with compromised membranes to fluoresce red ("dead"). Examination of individual induced or uninduced LIX32 (empty vector), LIX33 (pYA1611::$relE_{Mtb}$) and LIX34 (pYA1611::$relBE_{Mtb}$) cells demonstrated that 24 h post induction LIX32 and LIX34 cells appeared as normal, live, rod-shaped cells (Fig. 1A, top and bottom panels). In contrast, LIX33 cells post-induction underwent striking phenotypic changes that resulted in a heterogeneous population comprised of both normal bacilli and cells that possessed a large polar head, reminiscent of a spoon (Fig. 1A, middle panel). Additionally, cells overexpressing $relE_{Mtb}$ exhibited a "sticky" phenotype, apparent by the large cellular aggregates that formed despite exposure to a strong, nonionic detergent (Fig. 1A, middle panel). Both observations suggest that increased cellular levels of $RelE_{Mtb}$ induces cell envelope aberrations, which could result in both the "spoon" and "sticky" phenotypes.

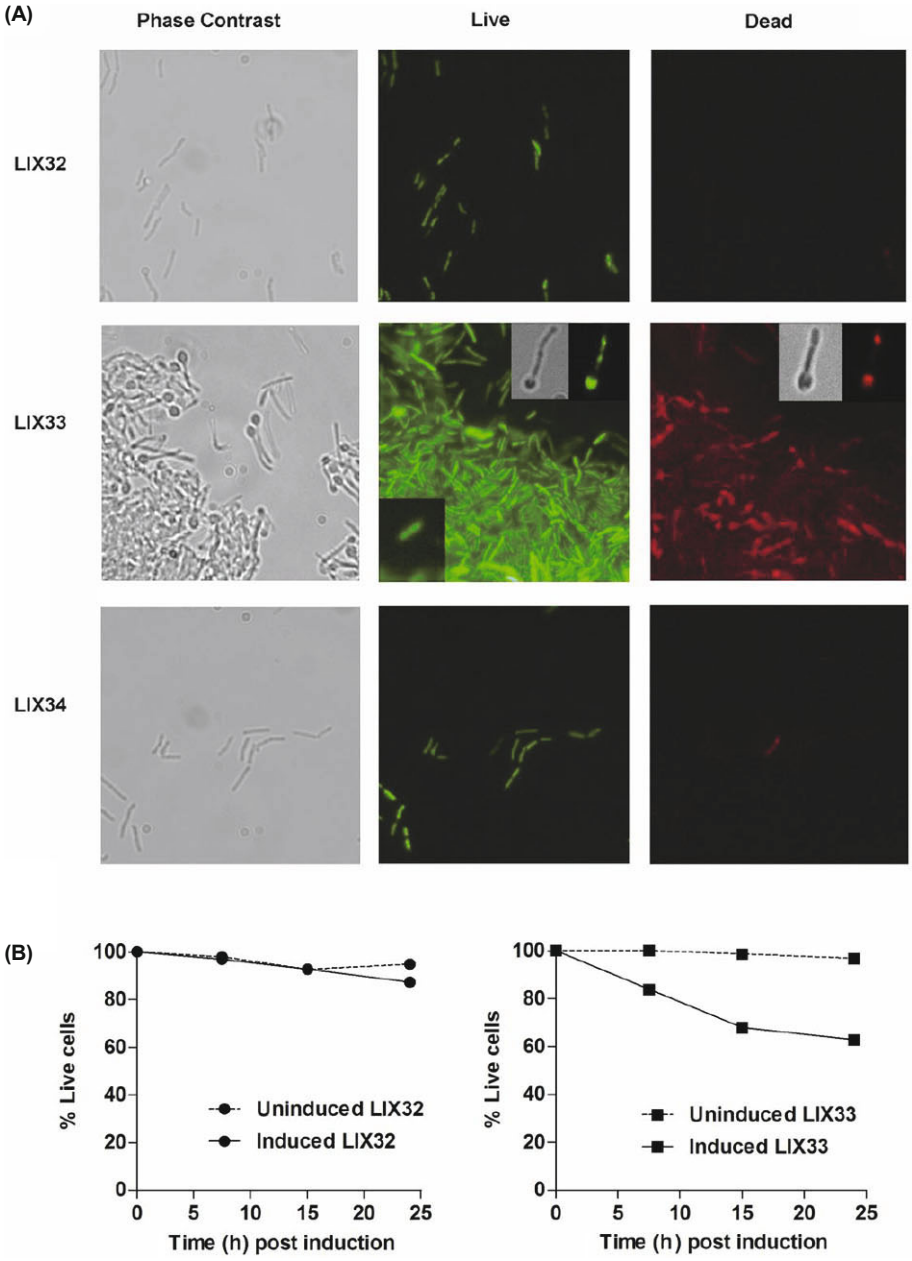

Fig. 1. $RelE_{Mtb}$ induces morphological and cell envelope changes in a genetically homogeneous population. Microscopic analysis of (A) LIX32 (pYA1611), upper panel; LIX33 (pYA1611::*relEMtb*), middle panel; and LIX34 (pYA1611::*relBEMtb*), lower panel, following 24 h of growth in inducing conditions. Cells were stained using a BacLight LIVE/DEAD bacterial viability kit (Molecular Probes, Invitrogen) and viewed using a fluorescent microscope. Live cells fluoresce green, whereas dead cells fluoresce red. For LIX32 and LIX34 the same field of view is shown for phase contrast, live and dead micrographs. For LIX33, the same field of view is shown for live and dead analysis, while a different field of view with fewer cells was chosen for the phase contrast micrograph. The lower left insert on the LIX33 live panel is a typical normal bacterium observed in LIX33 uninduced populations. The upper right insert for the LIX33 live panel are micrographs of the same cell observed for phase-contrast or fluorescent microscopy. The upper right insert for the LIX33 dead panel are micrographs of the same cell observed for phase-contrast or fluorescent microscopy. The cells shown for the live and dead inserts are from different fields and thus not the same bacterium. (B) Percentage of live cells in LIX32 (left) and LIX33 (right) cultures with time following addition of ATc. Single cell suspensions were stained using a BacLight LIVE/ DEAD kit and quantification of live and dead cells was achieved using a SpectraMax M2. Data is presented as the average of two independent replicates.

Fluorescent analysis revealed a mixed population of green and red-stained bacilli within the aggregates that assemble following *relE*$_{Mtb}$ over expression (Fig. 1A, LIX33, middle panel), indicating a loss of membrane integrity in a sub-population of cells, and potentially, a loss of viability. Of note, cells with an aberrant morphology could retain either the green or red stain, indicating that development of the polar head is not a predictor of membrane integrity (Fig. 1A, middle panel inset showing one live misshapen cell and a different dead misshapen cell). No alteration in shape or membrane integrity was observed when *relB*$_{Mtb}$ was co-expressed with *relE*$_{Mtb}$ (LIX34), demonstrating toxin neutralization (Fig. 1A, lower panel).

To determine the proportion of cells that exhibited a compromised envelope, induced and uninduced LIX32 and LIX33 cells were processed by aspiration to eliminate aggregates, and single cell suspensions were stained with SYTO-9 and PI followed by fluorometric quantification. The vast majority (96.9%) of the LIX32 population stained green ("live") 7.5 h post induction, with a slight reduction at 24 h (Fig. 1B, left graph). In contrast, the LIX33 population demonstrated reduced membrane integrity over time, with only 62.8% viability following 24 h of toxin expression (Fig. 1B, right graph). Considering the growth-inhibitory effects of RelE, these observations indicate that the presence of free RelE compromises the envelope structure, having negative implications on the viability of the bacilli, if the cells are unable to "fix" or "reseal" their membranes.

Ectopic RelE$_{Mtb}$ production inhibits growth via translation inhibition

E. coli K-12 has 10 type II TA modules where ectopic production of the toxin leads to a rapid degradation of mRNA and shut-down of translation (Pedersen *et al.*, 2003; Zhang, 2003; Jørgensen *et al.*, 2009). In *M. tuberculosis*, analysis of three MazF toxin proteins confirmed that each possesses mRNase activity, targeting unique "U-rich" recognition sequences (Zhu, 2008; Schifano *et al.*, 2013), while MazF-6 additionally possesses rRNase activity (Schifano *et al.*, 2013). In contrast, the *M. tuberculosis* VapC-mt4 toxin mediates translation inhibition through selective binding of RNA rather than from mRNA cleavage (Sharp *et al.*, 2012). In agreement with previous findings (Korch *et al.*, 2009), induction of *relE*$_{Mtb}$ in *M. smegmatis* significantly reduces growth (Fig. 2A). To analyze the effect of RelE$_{Mtb}$ on macromolecular synthesis with respect to growth reduction the incorporation of radioactive precursors into DNA ([^{3}H]-

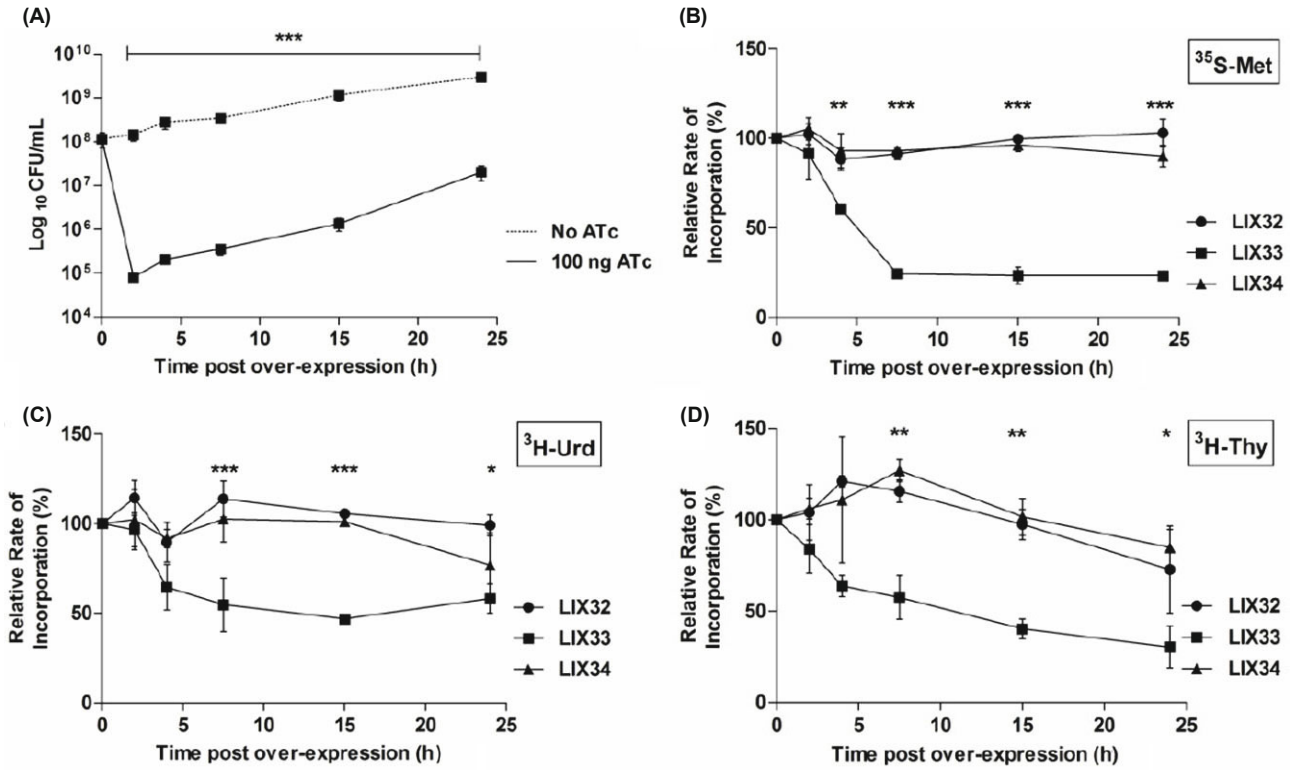

Fig. 2. Over expression of *relE*$_{Mtb}$ inhibits growth and macromolecular synthesis. *M. smegmatis* was transformed with either pYA1611 (LIX32), pYA1611::*relE* (LIX33) or pYA1611::*relBE* (LIX34). Overnight cultures were diluted to an OD_{600} of 0.01 in 7H9-Tw-Hyg. At an OD_{600} of 0.1, cultures were split, washed, resuspended in 7H9-Tw-Hyg and to one culture 100 ng/ml ATc was added to induce gene expression. (A) Growth of LIX33 with (solid line) and without (dashed line) ATc inducer. At the indicated time points uninduced LIX33 were diluted and plated on LB-agar, whereas induced LIX33 were plated on LB-ATc media. (B-D) Pulse-chase experiments were conducted to monitor the incorporation of radiolabeled precursors into (B) protein, [35S-Met], (C) RNA, [3H-Urd] or (D) DNA, [3H-Thy] with time. The incorporation rates are expressed as the percent relative to the incorporation of precursor into the uninduced culture at each time point. The values presented are the averages of three independent experiments; error bars represent the standard error of the mean. For statistical analysis, two-way analysis of variance with Bonferroni post tests was used to obtain *P* values for each time point *, $P < 0.05$; **, $P < 0.01$; ***, $P < 0.001$

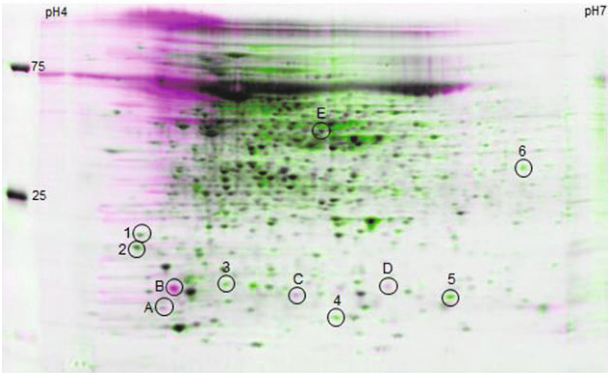

Fig. 3. Two-dimensional protein gel analysis of *M. smegmatis* over expressing *relE$_{Mtb}$* reveals global changes in the pattern of protein synthesis. LIX33 was grown as described for Fig. 2. At 24 h post induction, cells were harvested, proteins isolated and proteins separated by isoelectric focusing on pH 4–7 IPG strips in the first dimension, and 8–16% Tris-HCl SDS-PAGE in the second dimension. Proteins were visualized by Sypro Ruby staining and overlays of the gels made using Z3 gel analysis software. Pink spots (labeled A–E) represent proteins produced by induced LIX33; green spots (labeled 1–6) represent proteins produced by uninduced LIX33; black spots, proteins produced by both induced and uninduced LIX33. Numbered circles represent protein spots identified by mass spectrometry and their identities listed in Table 2. The positions of the standard protein size markers are indicated on the left, and pH gradient indicated across the top.

thymidine), RNA ([^{3}H]uridine), and protein ([^{35}S]methionine) was examined over time in *M. smegmatis* strains LIX32 (empty vector), LIX33 (pYA1611::*relE$_{Mtb}$*), and LIX34 (pYA1611::*relBE$_{Mtb}$*) (Fig. 2B–D). Shortly after induction of *relE$_{Mtb}$* (LIX33), methionine incorporation was reduced by 23% compared to the uninduced control (Fig. 2B, 4 h), at a time coincident with *relE$_{Mtb}$*-induced growth reduction (Fig. 2A). Significantly, following 7.5 h of *relE$_{Mtb}$* expression, translation rates decreased by 80% compared to the uninduced control, and remained at low levels for the remainder of the experiment. In comparison, RelE$_{Mtb}$ induced a more moderate reduction in transcription and DNA replication (compare 80% reduction in methionine incorporation at time 7.5 h, versus a 48% reduction in thymidine and 43% reduction in uridine), suggesting that RelE$_{Mtb}$ primarily targets translation. LIX32 and LIX34 exhibited high levels of methionine, thymidine and uridine incorporation (Fig. 2B–D), demonstrating that reduced macromolecular incorporation was due to RelE$_{Mtb}$ (LIX33) and that RelB$_{Mtb}$ (LIX34) is capable of neutralizing RelE$_{Mtb}$'s effects.

RelE$_{Mtb}$ induces proteomic alterations in mycobacteria

Unlike treatment with chloramphenicol, an antibiotic that completely inhibits mycobacterial translation (Robson *et al.*, 2009), protein synthesis was not entirely abolished by RelE$_{Mtb}$. The low level of translation (20%) remaining 24 h post *relE$_{Mtb}$* over expression suggests that a subset of proteins is protected from the effects of RelE$_{Mtb}$. To analyze the proteome and identify potential RelE$_{Mtb}$ targets, 2D gel protein analysis was performed on induced and uninduced LIX33 cells 24 h post *relE$_{Mtb}$* induction. We chose this time-point as the cells experience a significant shutdown of translation (Fig. 2B). As seen in Fig. 3, there is a distinct difference between the proteomic profiles of LIX33 over expressing *relE$_{Mtb}$* (pink spots, A–E) and cells not over expressing the toxin gene (green spots, 1–6). Determining the identity of proteins only present in uninduced LIX33 cultures was of particular interest, as we hypothesized the mRNA transcripts for these proteins could be cellular targets of RelE$_{Mtb}$. A subset of protein spots, from both induced and uninduced LIX33, were chosen for further analysis based on protein abundance and distance from neighboring protein spots. Using mass spectrometry, we identified potential RelE$_{Mtb}$-targets (Fig. 3 and Table 2): GarA (MSMEG_3467, spot 1), Chain A, MspA (MSMEG_0520, spot 2), hypothetical protein (MSMEG_2983, spot 3), Glyoxalase (MSMEG_6630, spot 4), ZbpA (MSMEG_2201, spot 5), and FabG (MSMEG_3150, spot 6), as well as pro-

Table 2. Identification of proteins absent following *relE$_{M.\ tb}$* induction

Spot no.	MSMEG ORF (Rv homologue)	Protein name	Gene function	No. of peptides matched	Sequence coverage (%)*
1	MSMEG_3647 (Rv1827)	GarA	modulates KGD[a] (inhibits), GS[b] (activates), GDH[c] (inhibits) (O'Hare *et al.*, 2008); regulator of glycogen degradation and glutamate metabolism (Alber, 2009)	1	9.3*
2	MSMEG_0520 (no Rv homologue)	MspA	Main porin in *M. smegmatis* for the uptake of small hydrophilic nutrients (Stahl *et al.*, 2001; Wolschendorf *et al.*, 2007), role in uptake of fluoroquinolone and chloramphenicol antibiotics (Danilchanka *et al.*, 2008)	1	7.6*
3	MSMEG_2983	hypothetical	Biological process unknown	2	25.2*
4	MSMEG_6630 (no Rv homologue; Rv0634c, Rv1637c, Rv3677c and Rv2581c are putative glyoxalases)	glyoxalase; putative glyoxalase family protein	Detoxifies keto-aldehydes such as methylglyoxal which participates in mycobacteria-induced cell apoptosis (Rachman *et al.*, 2006)	3	25.0*
5	MSMEG_2201 (Rv0130)	ZbpA	Homologous to Rv0130: FasII-like 3-hydroxyacyl-thioester dehydratase (Gurvitz *et al.*, 2008)	2	29.3*
6	MSMEG_3150 (Rv1483)	FabG; 3-oxoacyl-(acyl-carrier-protein) reductase	Functionally complements *M. tb* FabG1, catalyzes NADPH-specific reduction of long-chain ß-ketoacyl-ACP (C_8 to C_{20}); involved in the biosynthesis of mycolic acids (Marrakchi *et al.*, 2002; Parish *et al.*, 2007)	2	10.6*

* 99% confidence
[a] α-ketoglutarate decarboxylase
[b] glutamine synthetase
[c] glutamate dehydrogenase

teins present only following *relE*$_{Mtb}$ over expression (Fig. 3): hypothetical proteins (MSMEG_2983, spot A and MSMEG_2027, spot D), thioredoxin (MSMEG_3138, spot B), Hsp20/alpha-crystallin family (MSMEG_0424, spot C), acetyl-CoA transferase (MSMEG_4920, spot E).

RelE$_{Mtb}$ mediates mRNA interferase activity, degrading mycobacterial mRNA *in vivo*

To determine whether RelE$_{Mtb}$ directly affects protein synthesis of identified RelE$_{Mtb}$-targets, we used a cell-free in vitro transcription/translation assay programmed with target genes under the control of a T7 promoter with or without RelE$_{Mtb}$. Unlike other bacterial toxins that completely inhibit protein synthesis *in vitro*, the expression of *fabG*, *garA*, *gly*, and *zbpA* was not entirely inhibited by RelE$_{Mtb}$ in a cell-free system (Fig. 4A), but was reduced compared to reactions that didn't include RelE$_{Mtb}$. As a control for degradation, we similarly assayed the production of thioredoxin, a protein identified by mass spectrometry that was present following *relE* induction. As seen in Fig. 4, the production of thioredoxin was moderately influenced by *relE*$_{Mtb}$, but not to the extent observed for *fabG*, *garA*, *gly*, and *zbpA*. We were unable to determine whether RelB$_{Mtb}$ could neutralize the effects of RelE$_{Mtb}$ using the *in vitro* system due to protein instability. This result indicates that RelE$_{Mtb}$ reduced the translation of target proteins, but did not completely inhibit transcription or translation.

We speculate that the *in vitro* transcription/translation assay produces an insufficient amount of RelE$_{Mtb}$ and/or lacks *in vivo* co-factors or regulatory modifications that may be required for complete RelE$_{Mtb}$-directed inhibition of target gene expression and/or protein production. As a screen for *in vivo* degradation of *fabG*, *garA*, *gly*, *zbpA*, and *thioredoxin*, total RNA was isolated from LIX32 (empty vector) and LIX33 (*relE*$_{Mtb}$) 24 h post induction. RNA was reverse transcribed, and cDNA used as a template for PCR amplification using primers specific for full length *relE*, *fabG*, *garA*, *gly*, *zbpA*, and *thioredoxin* genes. Unexpectedly, amplification products were observed for *garA* and *fabG* regardless of cDNA template, suggesting that translation of GarA and FabG is inhibited by RelE$_{Mtb}$ in a manner that excludes mRNase degradation. With recent evidence demonstrating the cleavage of 23S and 16S rRNA by *M. tuberculosis* and *E. coli* MazF toxins (Vesper *et al.*, 2011; Schifano *et al.*, 2013, 2014) to generate specialized protein synthesis machinery, the reduction in protein synthesis following *relE*$_{Mtb}$ over expression without corresponding message degradation raises the potential for rRNase cleavage activity by RelE$_{Mtb}$. In support of RelE$_{Mtb}$ mRNase activity, both *gly* and *zbpA* message was detected in LIX32 cells not expressing the *relE* toxin gene (Fig. 4B, lane 1), but were absent following the induced expression of *relE* in LIX33 cells (Fig. 4B, lane 3). As further validation of our 2D-gel protein analysis, amplification of thioredoxin was only detected using LIX33 cDNA (data not shown). We hypothesize that our inability to PCR amplify *gly* or *zbpA* following *relE* induction (LIX33) is a result of *gly* and *zbpA* transcript degradation by RelE$_{Mtb}$.

To extend our observations and determine the *in vivo* activity of RelE$_{Mtb}$, primer extension was performed using RNA isolated from LIX32 and LIX33 cells 24 h post over expression of *relE*$_{Mtb}$ and primers specific for the *gly* gene. As seen in Fig. 4C, *gly* mRNA molecule is degraded following over expression of *relE*$_{Mtb}$. Specifically, two cleavage sites were observed at the 5′ end of *gly* mRNA near the translational start site, UCU↓CGC and CGC↓UCA (↓ denotes cleavage site, Fig. 4C). Each cleavage site was found in abundance in the *M. tuberculosis* genome (CGCUCA, 1383 sites; UCUCGC, 871 sites), and were specifically found in ORFs encoding *M. tuberculosis* proteins homologous to the *M. smegmatis* proteins identified in the 2D analysis. The absence of PCR amplification products for *gly* (Fig. 4B) and demon-

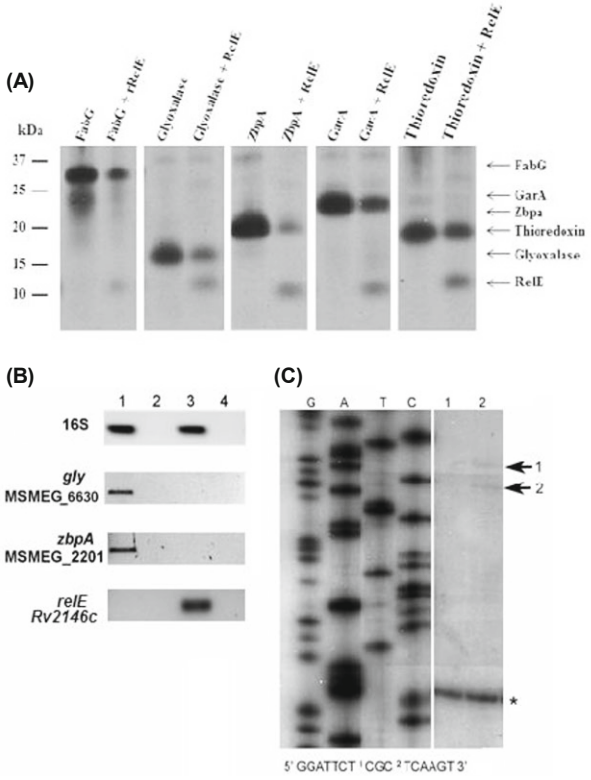

Fig. 4. RelE$_{Mtb}$ mediated mRNA cleavage *in vivo*. (A) A T7 S30 *in vitro* transcription/translation system was programmed with the DNA templates pET28::*relE*, pET28::*relB* and/or pET11::*target* (*fabG*/*garA*/*zpbA*/*thioredoxin*/*glyoxylase*). The positions of the individual proteins after SDS-15% PAGE are indicated. (B) Semi-quantitative analysis of mycobacterial transcripts in LIX32 (pYA1611) and LIX33 (pYA1611::*relE*) following 24 h of growth in inducing conditions as described for Fig. 2. RNA was harvested, reverse transcribed, and cDNA used as a template for PCR amplification using primers specific for full length *gly*, *zbpA*, and *relE* genes. All PCR amplifications were normalized to 16S RNA, thereby providing semi-quantitative data regarding the levels of transcript for each gene. Lanes: 1, LIX32 induced; 2, LIX32 induced without reverse transcriptase (-RT) control; 3, LIX33 induced; 4, LIX33 induced -RT control. (C) Primer extension of *gly* using RNA isolated from LIX32 and LIX33 after 24 h of induction and a gene-specific primer that annealed approximately 150 nt downstream of the translational start site. Lane 1 represents extension products obtained from LIX32, a control reaction where *relE*$_{Mtb}$ is not present; lane 2 represents extension products obtained from LIX33, where *relE*$_{Mtb}$ is present. Cleavage sites are indicated by numbered arrows. The sequences around the cleavage sites were determined using the RNA sequence ladders generated for *gly* mRNA using pYA1655 as a template and are indicated below the panels; the positions of the cleavage sites are indicated by numbers in the sequence. The presence of extension products for both LIX32 and LIX33 indicates that *gly* is expressed after 24 h of induction, in approximately equal quantities, and is indicated by an asterisk (*).

stration of cleavage sites for *gly* message (Fig. 4C) confirm a role for $RelE_{Mtb}$ *in vivo*, and suggest that $RelE_{Mtb}$ targets specific RNA sequences.

rel_{Mtb} toxin:antitoxin genes are differentially expressed in *M. tuberculosis* in response to environmental stresses

To ascertain the physiological relevance of the Rel_{Mtb} toxin: antitoxin family during mycobacterial growth and pathogenesis, we sought to identify the environments that caused transcriptional activation of all six *rel* genes. Thus, we analyzed the transcript levels of *relB*, *relE*, *relF*, *relG*, *relJ*, and *relK* in *M. tuberculosis* H37Rv under conditions of nitrogen limitation, carbon limitation, acidic pH, oxidative stress, and hypoxia in broth-grown cultures. For the conditions tested, each of the three rel_{Mtb} operons displayed similar up- and down-regulation patterns of expression, suggesting that they are responsive to stress conditions (Fig. 5). Using a nitrogen limitation model developed by Amon *et al.* (2008b), we determined that nitrogen stress elicited the most pronounced response for all six rel_{Mtb} genes, with a 30- to 40-fold increase in the transcription of *relF* and *relG* following 4 days of nitrogen stress (Fig. 5). Oxidative stress also induced the expression of rel_{Mtb} genes, with maximum up-regulation for *relK* (2.5-fold) over the no-stress control (Fig. 5), which agrees with previous findings by Singh *et al.* (2010). Unlike TA gene pairs *Rv2009-2010* (*vapBC*) and *Rv1955-1956* (*higBA*), whose expression is up-regulated during hypoxia (Ramage *et al.*, 2009), all six rel_{Mtb} genes were down-regulated in a hypoxic environment (Fig. 5). No significant change in rel_{Mtb} gene expression was observed during *M. tuberculosis* growth in carbon limited or acidic pH environments (Fig. 5). Taken together, these observations indicate that the rel_{Mtb} genes are differentially expressed under *in vitro* stress conditions and most importantly, highlight a role for Rel_{Mtb} toxin:antitoxin function under nitrogen-limiting and oxidative stress conditions.

Discussion

The genome of *M. tuberculosis* encodes an unusually high number of TA loci, whereas, in complete contrast, the genomes of mycobacteria outside of the *M. tuberculosis* complex (*M. africanum*, *M. bovis*, *M. canetti*, and *M. microti*) are virtually devoid of TA modules (Arcus *et al.*, 2005; Pandey and Gerdes, 2005; Ramage *et al.*, 2009). Bioinformatics analysis strongly supports the idea that TA gene expansion occurred after the *M. tuberculosis* complex and *M. marinum* diverged from their last common ancestor, supporting a role for these systems in the unique biology of the *M. tuberculosis* complex (Ramage *et al.*, 2009). To understand the contribution of TA modules towards *M. tuberculosis* pathogenicity, the independent actions of TA loci, the environmental conditions under which TA proteins are active, and the significance of toxin activity on the host cell must be established.

It has been demonstrated that stressors such as hypoxia, nutrient starvation, antibiotic exposure, macrophage infection and nitrosative and oxidative stress activate mycobacterial toxin:antitoxin gene expression (Korch *et al.*, 2009; Ramage *et al.*, 2009; Singh *et al.*, 2010; Halvorsen *et al.*, 2011; Albrethsen *et al.*, 2013). In agreement with Singh *et al*, we

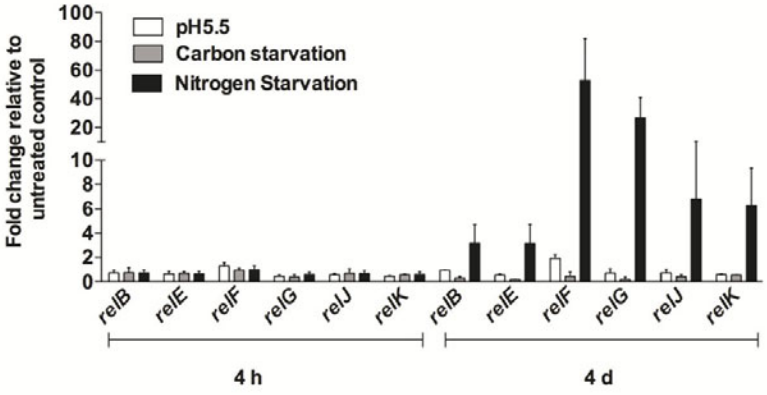

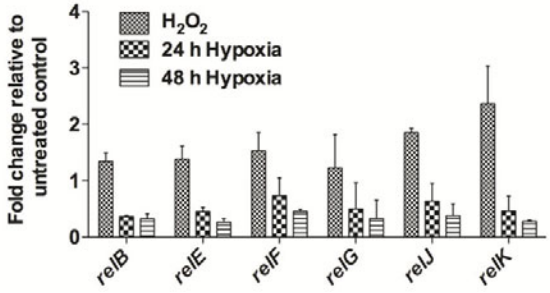

Fig. 5. *M. tuberculosis* rel_{Mtb} modules are differentially expressed upon exposure to *in vitro* environmental stress conditions. (A) qRT-PCR comparison of *relB*, *rel*E, *relF*, *relG*, *relJ*, and *relK* expression upon *M. tuberculosis* exposure to low pH (pH 5.5), carbon or nitrogen limiting environments, for 4 h or 4 d of stress exposure. Normalization of expression was done with respect to 16S rRNA expression and fold change of all six rel_{Mtb} genes in H37Rv grown under environmental stress conditions with respect to H37Rv grown in Middlebrook 7H7-Tween-ADS medium (untreated control) (baseline expression set to 1.0) is presented as the mean ± standard deviation of at least two independent experiments. (B) qRT-PCR analysis of *relB*, *relE*, *relF*, *relG*, *relJ*, and *relK* expression following *M. tuberculosis* exposure to 24 or 48 h hypoxic conditions or oxidative stress. Fold change of all six rel_{Mtb} genes in hypoxia or oxidative stress relative to the respective untreated control is presented as the mean ± standard deviation of at least two independent experiments.

observed an upregulation of all three rel_{Mtb} toxin genes under oxidative stress (Singh *et al.*, 2010). Here, our analysis further revealed that all three rel_{Mtb} antitoxins are similarly upregulated during states of oxidative stress. Our studies reveal an additional stress, nitrogen limitation, which significantly induces the expression of all six rel_{Mtb} genes in *M. tuberculosis,* particularly *relFG* (Fig. 5). Clearly, previous and current analysis of all three rel_{Mtb} modules unequivocally establishes that these are stress-responsive elements, but induction of these modules and the consequence of increased rel_{Mtb} expression relies on understanding toxin protein activity. In *E. coli*, the RelE toxin inhibits translation via the degradation of mRNA, however, the mRNA cleavage sites for $RelE_{E.coli}$ vary depending upon *in vivo* or *in vitro* assay conditions (Christensen and Gerdes, 2003; Pedersen *et al.*, 2003; Hurley *et al.*, 2011). Here we demonstrate that $RelE_{Mtb}$ inhibits translation, and specifically identify the Gly protein as a $RelE_{Mtb}$ target *in vivo* (Fig. 3) and *in vitro* (Fig. 4A), and established *in vivo* $RelE_{Mtb}$ cleavage sites within the mRNA coding region [TCT*CGC and CGC*TCA] (Fig. 4C). These sites are dissimilar to those described for $RelE_{E.coli}$, which could be due in part to assay conditions (*in vitro*, $RelE_{E.coli}$ versus *in vivo*, $RelE_{Mtb}$), as well as species characteristics such as GC content, cellular co-factors, pathogenicity and environmental niche. In support of species-specific toxin targets, the MazF toxin is characterized as an mRNA interferase in *E. coli*, *S. aureus* and *M. tuberculosis*, however, the recognition sequences are significantly different between the three species (Zhang, 2003, 2005; Muñoz-Gómez *et al.*, 2004; Zhu, 2008; Zhu *et al.*, 2009; Schifano *et al.*, 2013). This may explain why only a small subset of *M. tuberculosis mazEF* modules are functional in *E. coli* (Gupta, 2009).

Following $relE_{Mtb}$ expression *M. smegmatis*, we were unable to amplify transcripts encoding Gly or ZbpA proteins (Fig. 4B). However, using the *in vitro* transcription/translation assay, $RelE_{Mtb}$ reduced the production of Gly and ZbpA, but did not completely inhibit their production (Fig. 4A). One possible explanation is that the level of $RelE_{Mtb}$ protein generated within the system is below what is required for complete translation inhibition. In addition, we speculate that the *in vitro* assay lacks cellular co-factors or regulators that may be required for full toxin activity. Not surprisingly, we also observed effects of $RelE_{Mtb}$ on the mycobacterial proteome that were unrelated to mRNase activity. Unlike Gly or ZbpA, $RelE_{Mtb}$ inhibited the translation of FabG and GarA (Fig. 3) without targeting either transcript. Potentially, $RelE_{Mtb}$ possesses ribonuclease activity outside of the mRNA domain, to either rRNA or tRNA molecules, similar to VapC and MazF toxins in *E. coli* and *M. tuberculosis* (Vesper *et al.*, 2011; Winther and Gerdes, 2011; Schifano *et al.*, 2013; Winther *et al.*, 2013; Lopes *et al.*, 2014; Schifano *et al.*, 2014). Taken together, our data suggests that $RelE_{Mtb}$ inhibits translation via mRNA cleavage of specific target molecules *in vivo*, with additional consequences to protein production that are unrelated to mRNase activity.

An unexpected observation from our experimental analysis was that $RelE_{Mtb}$ encourages the development of large multicellular aggregates in *M. smegmatis*. Within these cell clumps are morphologically aberrant cells that possess a polar head, taking on a spoon-like appearance (Fig. 1A). It has recently been demonstrated that *Rv2866* (*relG*) causes mycobacterial cells to become filamentous (Miallau *et al.*, 2013), while the $VapC_{M.smegmatis}$ toxin potentiates the development of ovoid cells (Demidenok *et al.*, 2014). The polar expansion of mycobacterial cells following $relE_{Mtb}$ expression, and the elongation following *relG* expression, suggest that Rel_{Mtb} toxins impact lipid biosynthesis, cell envelope assembly, and/or cell division. In support of this, $RelE_{Mtb}$ inhibited the production of two key enzymes, ZpbA and FabG, involved in the biosynthesis of mycolic acids, a major fatty acid constituent found in mycobacterial cell envelopes (Fig. 3). *M. smegmatis* FabG can functionally complement *M. tuberculosis* FabG1 (Rv1483) (Parish *et al.*, 2007), which is essential for viability in *M. tuberculosis*. This correlates with our observation that $relE_{Mtb}$ over expression increased the probability of mycobacterial cell death, an inevitable consequence if stressed cells cannot reseal their damaged membrane (Fig. 1).

A defining and perplexing characteristic of *M. tuberculosis* is its ability to survive challenging environmental conditions and establish latent infections that can persist for decades. Toxin:antitoxin modules, particularly *hipBA* and *relBE*, have an established role in the transition of prokaryotes to a non-growing, persistent stage refractory to antibiotic exposure (Spoering and Lewis, 2001; Keren *et al.*, 2004; Korch and Hill, 2006; Möker *et al.*, 2010). In *M. tuberculosis*, *rel* toxin genes are upregulated in response to rifampin (*relE*, *relG*, *relK*), gentamycin (*relG* and *relK*) and levofloxacin (*relG* and *relK*) and contribute to antibiotic persistence and increased survival in a drug- and toxin-specific manner (Provvedi *et al.*, 2009; Singh *et al.*, 2010; Miallau *et al.*, 2013). In *E. coli*, $RelE_{E. coli}$ mediates tolerance to the bacteriocidal antibiotics ampicillin and ofloxacin in a density dependent manner (Tashiro *et al.*, 2012). Our studies revealed that following $relE_{Mtb}$ expression, cellular masses develop that are composed of cells in a live, dormant state, as well as cells that exhibit compromised cell membranes. Conceivably, in a crisis situation such as antibiotic exposure, nitrogen limitation or oxidative stress, the down regulation of growth by Rel_{Mtb} toxins enables cells to survive and persist long enough to bypass the stress. With that, given the outstanding number of TA modules encoded by *M. tuberculosis*, we anticipate that TA expression must be meticulously controlled to avoid superfluous initiation of the persistence program in favorable growth environments.

Competing interests

The authors declare that they have no competing interests.

Author's contributions

SBK performed the live/dead analysis, primer extension, two-dimensional PAGE, *in vitro* T7/S30 transcription translation assay, growth of *M. tuberculosis* in stress conditions and drafted the manuscript. VM performed RNA isolation and qRT-PCR analysis. HC performed the pulse-chase experiments. JCC contributed to the overall study design. All authors read, edited and approved the final manuscript.

Acknowledgements

Mass spectrometry was performed at the Michigan Proteome Consortium, University of Michigan. We thank Mary Hurley and Angela Walker for assistance with the generation and analysis of mass spectrometry data. H.C. was supported by the Arizona State University PREP Program for Biomedical Research and Public Health Service grant GM071798 from the U.S. National Institutes of Health. This research was supported by Public Health Services grant AI46428 from the U.S. National Institutes of Health awarded to J.E.C-C.

References

Alber, T. 2009. Signaling mechanisms of the *Mycobacterium tuberculosis* receptor Ser/Thr protein kinases. *Curr. Opin. Struct. Biol.* **19**, 650–657.

Albrethsen, J., Agner, J., Piersma, S.R., Højrup, P., Pham, T.V., Weldingh, K., Jimenez, C.R., Andersen, P., and Rosenkrands, I. 2013. Proteomic profiling of *Mycobacterium tuberculosis* identifies nutrient-starvation-responsive toxin-antitoxin systems. *Mol. Cell. Proteomics* **12**, 1180–1191.

Amitai, S., Kolodkin-Gal, I., Hananya-Meltabashi, M., Sacher, A., and Engelberg-Kulka, H. 2009. *Escherichia coli* MazF leads to the simultaneous selective synthesis of both death and survival proteins. *PLoS Genet.* **5**, e1000390.

Amon, J., Brau, T., Grimrath, A., Hanssler, E., Hasselt, K., Holler, M., Jessberger, N., Ott, L., Szokol, J., Titgemeyer, F., *et al.* 2008a. Nitrogen control in *Mycobacterium smegmatis*: nitrogen-dependent expression of ammonium transport and assimilation proteins depends on the OmpR-Type regulator GlnR. *J. Bacteriol.* **190**, 7108–7116.

Amon, J., Titgemeyer, F., and Burkovski, A. 2008b. A genomic view on nitrogen metabolism and nitrogen control in mycobacteria. *J. Mol. Microbiol. Biotechnol.* **17**, 20–29.

Arcus, V.L., Rainey, P.B., and Turner, S.J. 2005. The PIN-domain toxin-antitoxin array in mycobacteria. *Trends Microbiol.* **13**, 360–365.

Blower, T.R., Short, F.L., Rao, F., Mizuguchi, K., Pei, X.Y., Fineran, P.C., Luisi, B.F., and Salmond, G.P.C. 2012. Identification and classification of bacterial Type III toxin-antitoxin systems encoded in chromosomal and plasmid genomes. *Nucleic Acids Res.* doi: 10.1093/nar/gks231.

Christensen, S.K. and Gerdes, K. 2003. RelE toxins from bacteria and archaea cleave mRNAs on translating ribosomes, which are rescued by tmRNA. *Mol. Microbiol.* **48**, 1389–1400.

Christensen, S.K., Pedersen, K., Hansen, F.G., and Gerdes, K. 2003. Toxin-antitoxin loci as stress-response-elements: ChpAK/MazF and ChpBK cleave translated RNAs and are counteracted by tmRNA. *J. Mol. Biol.* **332**, 809–819.

Christensen-Dalsgaard, M. and Gerdes, K. 2008. Translation affects YoeB and MazF messenger RNA interferase activities by different mechanisms. *Nucleic Acids Res.* **36**, 6472–6481.

Danilchanka, O., Pavlenok, M., and Niederweis, M. 2008. Role of porins for uptake of antibiotics by *Mycobacterium smegmatis*. *Antimicrob. Agents Chemother.* **52**, 3127–3134.

Demidenok, O.I., Kaprelyants, A.S., and Goncharenko, A.V. 2014. Toxin-antitoxin vapBC locus participates in formation of the dormant state in *Mycobacterium smegmatis*. *FEMS Microbiol. Lett.* **352**, 69–77.

Engelberg-Kulka, H., Amitai, S., Kolodkin-Gal, I., and Hazan, R. 2006. Bacterial programmed cell death and multicellular behavior in bacteria. *PLoS Genet.* **2**, e135.

Fozo, E.M., Makarova, K.S., Shabalina, S.A., Yutin, N., Koonin, E.V., and Storz, G. 2010. Abundance of type I toxin-antitoxin systems in bacteria: searches for new candidates and discovery of novel families. *Nucleic Acids Res.* **38**, 3743–3759.

Fu, Z., Tamber, S., Memmi, G., Donegan, N.P., and Cheung, A.L. 2009. Overexpression of MazFSa in *Staphylococcus aureus* induces bacteriostasis by selectively targeting mRNAs for cleavage. *J. Bacteriol.* **191**, 2051–2059.

Gerdes, K., Christensen, S.K., and Lobner-Olesen, A. 2005. Prokaryotic toxin-antitoxin stress response loci. *Nat. Rev. Microbiol.* **3**, 371–382.

Gerdes, K., Rasmussen, P.B., and Molin, S. 1986. Unique type of plasmid maintenance function: postsegragational killing of plasmid-free cells. *Proc. Natl. Acad. Sci. USA* **83**, 3116–3120.

Germain, E., Castro-Roa, D., Zenkin, N., and Gerdes, K. 2013. Molecular mechanism of bacterial persistence by HipA. *Mol. Cell* **52**, 248–254.

Goeders, N., Drèze, P.L., and Van Melderen, L. 2013. Relaxed cleavage specificity within the RelE toxin family. *J. Bacteriol.* **195**, 2541–2549.

Gupta, A. 2009. Killing activity and rescue function of genome-wide toxin-antitoxin loci of *Mycobacterium tuberculosis*. *FEMS Microbiol. Lett.* **290**, 45.

Gurvitz, A., Hiltunen, J.K., and Kastaniotis, A.J. 2008. Identification of a novel mycobacterial 3-hydroxyacyl-thioester dehydratase, HtdZ (Rv0130), by functional complementation in yeast. *J. Bacteriol.* **190**, 4088–4090.

Hallez, R., Geeraerts, D., Sterckx, Y., Mine, N., Loris, R., and Van Melderen, L. 2010. New toxins homologous to ParE belonging to three-component toxin-antitoxin systems in *Escherichia coli* O157:H7. *Mol. Microbiol.* **76**, 719–732.

Halvorsen, E.M., Williams, J.J., Bhimani, A.J., Billings, E.A., and Hergenrother, P.J. 2011. Txe, an endoribonuclease of the enterococcal Axe-Txe toxin-antitoxin system, cleaves mRNA and inhibits protein synthesis. *Microbiology* **157**, 387–397.

Harth, G.a.M.A.H. 1999. An inhibitor of exported *Mycobacterium tuberculosis* glutamine synthetase selectively blocks the growth of pathogenic mycobacteria in axenic culture and in human monocytes: extracellular proteins ad potential novel drug targets. *J. Exp. Med.* **189**, 1425–1435.

Hurley, J.M., Cruz, J.W., Ouyang, M., and Woychik, N.A. 2011. Bacterial toxin RelE mediates frequent codon-independent mRNA cleavage from the 5′ end of coding regions *in vivo*. *J. Biol. Chem.* **286**, 14770–14778.

Hurley, J.M. and Woychik, N.A. 2009. Bacterial toxin HigB associates with ribosomes and mediates translation-dependent mRNA cleavage at A-rich sites. *J. Biol. Chem.* **284**, 18605–18613.

Jensen, R.B. and Gerdes, K. 1995. Programmed cell death in bacteria: proteic plasmid stabilization systems. *Mol. Microbiol.* **17**, 205–210.

Jiang, U., Pogliano, J., Helinski, D.R., and Konieczny, I. 2002. ParE toxin encoded by the broad-host-range plasmid RK2 is an inhibitor of *Escherichia coli* gyrase. *Mol. Microbiol.* **44**, 971–979.

Jørgensen, M.G., Pandey, D.P., Jaskolska, M., and Gerdes, K. 2009. HicA of *Escherichia coli* defines a novel family of translation-independent mRNA interferases in bacteria and Archaea. *J. Bacteriol.* **191**, 1191–1199.

Kaspy, I., Rotem, E., Weiss, N., Ronin, I., Balaban, N.Q., and Glaser, G. 2013. HipA-mediated antibiotic persistence via phosphorylation of the glutamyl-tRNA-synthetase. *Nat. Commun.* **4**, doi: 10.1038/ncomms4001.

Keren, I., Kaldalu, N., Spoering, A., Wang, Y., and Lewis, K. 2004. Persister cells and tolerance to antimicrobials. *FEMS Microbiol. Lett.* **230**, 13.

Korch, S.B., Contreras, H., and Clark-Curtiss, J.E. 2009. Three *Mycobacterium tuberculosis* Rel toxin-antitoxin modules inhibit mycobacterial growth and are expressed in infected human macrophages. *J. Bacteriol.* **191**, 1618–1630.

Korch, S.B., Henderson, T., and Hill, T.M. 2003. Characterization

of the *hipA7* allele of *Escherichia coli* and evidence that high persistence is governed by (p)ppGpp synthesis. *Mol. Microbiol.* **50**, 1199–1213.

Korch, S.B. and Hill, T.M. 2006. Ectopic overexpression of wild-type and mutant *hipA* genes in *Escherichia coli*: Effects on macromolecular synthesis and persister formation. *J. Bacteriol.* **188**, 3826–3836.

Leplae, R., Geeraerts, D., Hallez, R., Guglielmini, J., Drèze, P., and Van Melderen, L. 2011. Diversity of bacterial type II toxin-antitoxin systems: a comprehensive search and functional analysis of novel families. *Nucleic Acids Res.* **39**, 5513–5525.

Lopes, A.P.Y., Lopes, L.M., Fraga, T.R., Chura-Chambi, R.M., Sanson, A.L., Cheng, E., Nakajima, E., Morganti, L., and Martins, E.A.L. 2014. VapC from the leptospiral VapBC toxin-antitoxin module displays ribonuclease activity on the initiator tRNA. *PLoS One* **9**, e101678.

Maisonneuve, E. and Gerdes, K. 2014. Molecular mechanisms underlying bacterial persisters. *Cell* **157**, 539–548.

Malhotra, V., Arteaga-Cortes, L.T., Clay, G., and Clark-Curtiss, J.E. 2010. *Mycobacterium tuberculosis* protein kinase K confers survival advantage during early infection in mice and regulates growth in culture and during persistent infection: implications for immune modulation. *Microbiology* **156**, 2829–2841.

Malhotra, V., Tyagi, J.S., and Clark-Curtiss, J.E. 2009. DevR-mediated adaptive response in *Mycobacterium tuberculosis* H37Ra: Links to asparagine metabolism. *Tuberculosis* **89**, 169.

Marrakchi, H., Ducasse, S., Labesse, G., Montrozier, H., Margeat, E., Emorine, L., Charpentier, X., Daffe, M., and Quemard, A. 2002. MabA (FabG1), a *Mycobacterium tuberculosis* protein involved in the long-chain fatty acid elongation system FAS-II. *Microbiology* **148**, 951–960.

Miallau, L., Jain, P., Arbing, M.A., Cascio, D., Phan, T., Ahn, C.J., Chan, S., Chernishof, I., Maxson, M., Chiang, J., *et al.* 2013. Comparative proteomics identifies the cell-associated lethality of *M. tuberculosis* RelBE-like toxin-antitoxin complexes. *Structure* **21**, 627–637.

Möker, N., Dean, C.R., and Tao, J. 2010. *Pseudomonas aeruginosa* increases formation of multidrug-tolerant persister cells in response to quorum-sensing signaling molecules. *J. Bacteriol.* **192**, 1946–1955.

Muñoz-Gómez, A.J., Santos-Sierra, S., Berzal-Herranz, A., Lemonnier, M., and Díaz-Orejas, R. 2004. Insights into the specificity of RNA cleavage by the *Escherichia coli* MazF toxin. *FEBS Lett.* **567**, 316–320.

Nariya, H. and Inouye, M. 2008. MazF, an mRNA interferase, mediates programmed cell death during multicellular *Myxococcus* development. *Cell* **132**, 55–66.

Neubauer, C., Gao, Y.G., Andersen, K.R., Dunham, C.M., Kelley, A.C., Hentschel, J., Gerdes, K., Ramakrishnan, V., and Brodersen, D.E. 2009. The structural basis for mRNA recognition and cleavage by the ribosome-dependent endonuclease RelE. *Cell* **139**, 1084–1095.

O'Hare, H.M., Durán, R., Cerveñansky, C., Bellinzoni, M., Wehenkel, A.M., Pritsch, O., Obal, G., Baumgartner, J., Vialaret, J., Johnsson, K., *et al.* 2008. Regulation of glutamate metabolism by protein kinases in mycobacteria. *Mol. Microbiol.* **70**, 1408–1423.

Orgura, T. and Hiraga, S. 1983. Mini-F plasmid genes that couple host cell division to plasmid proliferation. *Proc. Natl. Acad. Sci. USA* **80**, 4784–4788.

Pandey, D.P. and Gerdes, K. 2005. Toxin-antitoxin loci are highly abundant in free-living but lost from host-associated prokaryotes. *Nucleic Acids Res.* **33**, 966–976.

Parish, T., Roberts, G., Laval, F., Schaeffer, M., Daffe, M., and Duncan, K. 2007. Functional complementation of the essential gene *fabG1* of *Mycobacterium tuberculosis* by *Mycobacterium smegmatis fabG* but not *Escherichia coli fabG*. *J. Bacteriol.* **189**, 3721–3728.

Pedersen, K., Zavialov, A.V., Pavlov, M.Y., Elf, J., Gerdes, K., and Ehrenberg, M. 2003. The bacterial toxin RelE displays codon-specific cleavage of mRNAs in the ribosomal A site. *Cell* **112**, 131–140.

Provvedi, R., Boldrin, F., Falciani, F., Palù, G., and Manganelli, R. 2009. Global transcriptional response to vancomycin in *Mycobacterium tuberculosis*. *Microbiology* **155**, 1093–1102.

Prysak, M.H., Mozdzierz, C.J., Cook, A.M., Zhu, L., Zhang, Y., Inouye, M., and Woychik, N.A. 2009. Bacterial toxin YafQ is an endoribonuclease that associates with the ribosome and blocks translation elongation through sequence-specific and frame-dependent mRNA cleavage. *Mol. Microbiol.* **71**, 1071–1087.

Rachman, H., Kim, N., Ulrichs, T., Baumann, S., Pradl, L., Eddine, A.N., Bild, M., Rother, M., Kuban, R.J., Lee, J.S., *et al.* 2006. Critical role of methylglyoxal and AGE in mycobacteria-induced macrophage apoptosis and activation. *PLoS One* **1**, e29.

Ramage, H.R., Connolly, L.E., and Cox, J.S. 2009. Comprehensive functional analysis of *Mycobacterium tuberculosis* toxin-antitoxin systems: implications for pathogenesis, stress responses, and evolution. *PLoS Genet.* **5**, e1000767.

Robson, J., McKenzie, J.L., Cursons, R., Cook, G.M., and Arcus, V.L. 2009. The *vapBC* operon from *Mycobacterium smegmatis* is an autoregulated toxin-antitoxin module that controls growth via inhibition of translation. *J. Mol. Biol.* **390**, 353–367.

Saini, D.K., Malhotra, V., Dey, D., Pant, N., Das, T.K., and Tyagi, J.S. 2004. DevR-DevS is a bona fide two-component system of *Mycobacterium tuberculosis* that is hypoxia-responsive in the absence of the DNA-binding domain of DevR. *Microbiology* **150**, 865–875.

Sambrook, J., Fritsch, E.F., and Maniatis, T. 1989. Molecular cloning: a laboratory manual. Cold Spring Harbor Laboratory, Cold Spring Harbor, New York, USA.

Schifano, J.M., Edifor, R., Sharp, J.D., Ouyang, M., Konkimalla, A., Husson, R.N., and Woychik, N.A. 2013. Mycobacterial toxin MazF-mt6 inhibits translation through cleavage of 23S rRNA at the ribosomal A site. *Proc. Natl. Acad. Sci. USA* **110**, 8501–8506.

Schifano, J.M., Vvedenskaya, I.O., Knoblauch, J.G., Ouyang, M., Nickels, B.E., and Woychik, N.A. 2014. An RNA-seq method for defining endoribonuclease cleavage specificity identifies dual rRNA substrates for toxin MazF-mt3. *Nat. Commun.* **5**, 3538.

Sharp, J.D., Cruz, J.W., Raman, S., Inouye, M., Husson, R.N., and Woychik, N.A. 2012. Growth and translation inhibition through sequence-specific RNA binding by *Mycobacterium tuberculosis* VapC toxin. *J. Biol. Chem.* **287**, 12835–12847.

Singh, R., Barry, C.E., III, and Boshoff, H.I.M. 2010. The three RelE homologs of *Mycobacterium tuberculosis* have individual, drug-specific effects on bacterial antibiotic tolerance. *J. Bacteriol.* **192**, 1279–1291.

Snapper, S.B., Melton, R.E., Mustafa, S., Keiser, T., and Jacobs, W.R.Jr. 1990. Isolation and characterization of efficient plasmid transformation mutants of *Mycobacterium smegmatis*. *Mol. Microbiol.* **4**, 1911–1999.

Spoering, A.L. and Lewis, K. 2001. Biofilms and planktonic cells of *Pseudomonas aeruginosa* have similar resistance to killing by antimicrobials. *J. Bacteriol.* **183**, 6746–6751.

Stahl, C., Kubetzko, S., Kaps, I., Seeber, S., Engelhardt, H., and Niederweis, M. 2001. MspA provides the main hydrophilic pathway through the cell wall of *Mycobacterium smegmatis*. *Mol. Microbiol.* **40**, 451–464.

Tashiro, Y., Kawata, K., Taniuchi, A., Kakinuma, K., May, T., and Okabe, S. 2012. RelE-mediated dormancy is enhanced at high cell density in *Escherichia coli*. *J. Bacteriol.* **194**, 1169–1176.

Tiwari, P., Arora, G., Singh, M., Kidwai, S., Narayan, O.P., and Singh, R. 2015. MazF ribonucleases promote *Mycobacterium tuberculosis* drug tolerance and virulence in guinea pigs. *Nat. Commun.* **6**, 6059.

Tripathi, A., Dewan, P.C., Siddique, S.A., and Varadarajan, R. 2014. MazF-induced growth inhibition and persister generation in

Escherichia coli. *J. Biol. Chem.* **289**, 4191–4205.

Tsuchimoto, S., Ohtsubo, H., and Ohtsubo, E. 1988. Two genes, *pemK* and *pemI*, responsible for stable maintenance of resistance plasmid R100. *J. Bacteriol.* **170**, 1461–1466.

Vesper, O., Amitai, S., Belitsky, M., Byrgazov, K., Kaberdina, A.C., Engelberg-Kulka, H., and Moll, I. 2011. Selective translation of leaderless mRNAs by specialized ribosomes generated by MazF in *Escherichia coli*. *Cell* **147**, 147–157.

Winther, K.S., Brodersen, D.E., Brown, A.K., and Gerdes, K. 2013. VapC20 of *Mycobacterium tuberculosis* cleaves the Sarcin-Ricin loop of 23S rRNA. *Nat. Commun.* **4**, 2796.

Winther, K.S. and Gerdes, K. 2011. Enteric virulence associated protein VapC inhibits translation by cleavage of initiator tRNA. *Proc. Natl. Acad. Sci. USA* **108**, 7403–7407.

Wolschendorf, F., Mahfoud, M., and Niederweis, M. 2007. Porins are required for uptake of phosphates by *Mycobacterium smegmatis*. *J. Bacteriol.* **189**, 2435–2442.

Yamaguchi, Y., Park, J.H., and Inouye, M. 2009. MqsR, a crucial regulator for quorum sensing and biofilm formation, is a GCU-specific mRNA interferase in *Escherichia coli*. *J. Biol. Chem.* **284**, 28746–28753.

Yang, M., Gao, C., Wang, Y., Zhang, H., and He, Z.G. 2010. Characterization of the interaction and cross-regulation of three *Mycobacterium tuberculosis* RelBE modules. *PLoS One* **5**, e10672.

Zhang, Y. and Inouye, M. 2009. The inhibitory mechanism of protein synthesis by YoeB, an *Escherichia coli* toxin. *J. Biol. Chem.* **284**, 6627–6638.

Zhang, Y., Zhang, J., Hara, H., Kato, I., and Inouye, M. 2005. Insights into the mRNA cleavage mechanism by MazF, an mRNA interferase. *J. Biol. Chem.* **280**, 3143–3150.

Zhang, Y., Zhang, J., Hoeflich, K.P., Ikura, M., Qing, G., and Inouye, M. 2003. MazF cleaves cellular mRNAs specifically at ACA to block protein synthesis in *Escherichia coli*. *Mol. Cell* **12**, 913–923.

Zhu, L., Inoue, K., Yoshizumi, S., Kobayashi, H., Zhang, Y., Ouyang, M., Kato, F., Sugai, M., and Inouye, M. 2009. *Staphylococcus aureus* MazF specifically cleaves a pentad sequence, UACAU, which is unusually abundant in the mRNA for pathogenic adhesive factor SraP. *J. Bacteriol.* **191**, 3248–3255.

Zhu, L., Phadtare, S., Nariya, H., Ouyang, M., Husson, R.N., and Inouye, M. 2008. The mRNA interferases, MazF-mt3 and MazF-mt7 from *Mycobacterium tuberculosis* target unique pentad sequences in single-stranded RNA. *Mol. Microbiol.* **69**, 559–569.